Intershell and intersubshell effects in photoionization of atoms

M. Ya. Amus'ya, V. K. Ivanov, N. A. Cherepkov, and L. V. Chernysheva

A. F. Ioffe Physico-technical Institute, USSR Academy of Sciences
(Submitted May 10, 1973; resubmitted October 30, 1973)
Zh. Eksp. Teor. Fiz. 66, 1537–1549 (May 1974)

Partial photoionization cross sections for weak transitions in a number of atoms have been obtained taking intershell interaction into account. It is shown that the effect of neighboring many-electron shells or subshells can lead to a qualitatively new behavior of the photoabsorption cross section. Three cases are considered: 1) the effect of an outer subshell on the photoionization of an inner shell —photoionization of s^2 subshells of noble gas atoms, 2) the effect of an inner shell on an outer one —photoionization of $4s^2$ subshells in Ca and Zn, and 3) the effect of an inner shell near its ionization threshold on outer shells—the single ionization cross section for Kr and Xe near the d^{10}-subshell thresholds. In all cases agreement with experiment is improved.

1. INTRODUCTION

At the present time there exist experimental possibilities for obtaining exhaustive information concerning the partial contributions to the photoionization cross section of different transitions both of the principal ones giving the main contribution to the total cross section, and also of the weak ones[1], and concerning their influence on each other.

Theoretical calculations of the total photoabsorption cross section have shown that its magnitude is determined by the main transition[2] $l \to l+1$ (l is the orbital angular momentum of the electron undergoing ionization). It was also shown that within the framework of this transition correlations between electrons are strong[3]. In the latter calculations the mutual influence of the weak and the strong transitions on each other has been neglected. However, one can expect that weak transitions are to a great extent subject to being influenced by the other transitions. This must be taken into account in obtaining partial cross sections[4,5]. The corresponding effect must be stronger the greater is the amplitude of the transition which exercises this influence, and the closer to each other in energy are situated the shells or the subshells transitions from which are being investigated.

In the present paper a study is made for the first time of the effect of the intershell interaction on the probabilities of different partial transitions. It is shown that taking this interaction into account has a significant effect on the value of the cross section for the weak transition, and sometimes even alters the nature of its behavior. An investigation is made both of the effect of an outer shell on the photoionization of a deeper one, and also of the effect of inner shells on the photoionization of outer ones. The photoionization cross section is calculated for the outer ns^2 subshells (n is the principal quantum number) of noble gas atoms taking into account the effect of the np^6 subshell and a qualitatively new behavior of the cross section is found compared to the single-particle cross section. The photoionization cross section for the $4s^2$ electrons of Ca and Zn has been calculated taking into account the effect of the inner subshells $3p^6$ in Ca and $3d^{10}$ in Zn. In both cases the effect of the neighboring subshell leads to strong screening of the outer one from external action (an incident quantum). The interaction with an inner d-shell near its threshold has a decisive effect on the process of ionization of outer shells $4s^24p^6$ of Kr and $5s^25p^6$ of Xe. In the case of Xe it leads to a quite sharp maximum in the ionization cross section of the outer shell in the neighborhood of the threshold of the inner $4d^{10}$ subshell.

2. CALCULATION OF THE PHOTOIONIZATION CROSS SECTION

In order to calculate the contribution to the photoionization cross section determined by the transition of an electron from the state n_1l_1 to the state n_2l_2 we make use of the expression[6] ($\hbar = m = e = 1$):

$$\sigma^{(r)}_{n_1l_1\to n_2l_2}(\omega) = 4\pi^2\alpha a_0^2 \frac{N_{n_1l_1}}{2l_1+1}\omega |\langle n_2l_2|\hat{d}_r|n_1l_1\rangle|^2, \tag{1}$$

where $4\pi^2\alpha a_0^2 = 8.067\times 10^{-18}$ cm^2, N_{nl} is the number of electrons in the nl subshell, ω is the energy of the incident quantum, $\langle n_2l_2|\hat{\mathbf{d}}_\mathbf{r}|n_1l_1\rangle$ is the dipole matrix element evaluated using the operator $\mathbf{r}$. In the random phase approximation with exchange within the framework of a single transition ($n_1l_1 \to n_2l_2$) in order to determine the dipole matrix element the following integral equation[3] is solved

$$\langle n_2l_2|\hat{D}|n_1l_1\rangle = \langle n_2l_2|\hat{d}|n_1l_1\rangle + \Big(\sum_{\substack{n_3>F\\ n_4=n_1}} - \sum_{\substack{n_4>F\\ n_3=n_1}}\Big)\frac{\langle n_3l_3|\hat{D}|n_4l_4\rangle\langle n_4l_4, n_2l_2|\hat{U}|n_3l_3, n_1l_1\rangle}{\omega-(E_{n_3}-E_{n_4})+i\delta(1-2n_{n_3})}. \tag{2}$$

In this equation the matrix element of the Coulomb interaction $\langle\hat{U}\rangle$ is diagonal with the respect to the hole state n_1l_1.

We consider the amplitude for the dipole transition from the subshell n_1l_1 taking into account the interaction with the transition from the subshell n_il_i without going outside the framework of the random phase approximation including exchange (RPAE). We restrict ourselves to perturbation theory of the first order with respect to the interaction between the transitions—the intershell interaction. Starting with[3] one can obtain the formula for the photoionization cross section of the n_1l_1 subshell:

$$\sigma^{(r)}_{n_1l_1\to n_2l_2}(\omega) = 4\pi^2\alpha a_0^2 \frac{N_{n_1l_1}}{2l_1+1}\omega \Big| \langle n_2l_2|\hat{D}_r|n_1l_1\rangle + \Big(\sum_{\substack{n_4>F\\ n_3=n_i}} - \sum_{\substack{n_3>F\\ n_4=n_i}}\Big)\frac{\langle n_4l_4|\hat{D}_r|n_3l_3\rangle\langle n_3l_3, n_2l_2|\hat{\Gamma}|n_4l_4, n_1l_1\rangle}{\omega-(E_{n_4}-E_{n_3})+i\delta(1-2n_{n_4})}\Big|^2. \tag{3}$$

The amplitude entering into (3) is graphically represented in Fig. 1. The first term $\langle\hat{D}_\mathbf{r}\rangle$ describes the direct transition from the n_1l_1 subshell taking into account correlations within the framework of this

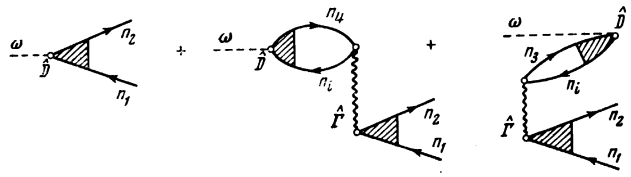

FIG. 1. The amplitude for the phototransition $n_1l_1 \to n_2l_2$ taking into account the effect of the n_il_i subshell. The solid line with an arrow directed to the right corresponds to a particle, with an arrow to the left corresponds to a hole, the dotted line corresponds to an incident quantum of energy ω, while the wavy line corresponds to the Coulomb interaction between electrons. The shaded triangle taking correlations into account within the framework of one transition.

$(n_1l_1 \to n_2l_2)$ transition, i.e., it is obtained from equation (2). The second term represents the amplitude for the photoionization of the n_1l_1 subshell taking into account the effect of the transition from the n_il_i subshell, i.e., it describes a two-stage process in which the incident quantum at first virtually excites the n_il_i electrons, and then the latter transfer the excitation to the electrons of the n_1l_1 subshell. Here, $\langle n_4l_4|D_r|n_3l_3\rangle$ is the dipole matrix element for a transition from the n_il_i subshell. It is also obtained from equation (2). The matrix element $\langle\hat{\Gamma}\rangle$ describes the interaction between two transitions taking into account the correlations within the framework of the $(n_1l_1 \to n_2l_2)$ transition under consideration and is obtained from an equation similar to (2):

$$\langle n_3l_3, n_2l_2|\hat{\Gamma}|n_il_i, n_1l_1\rangle = \langle n_3l_3, n_2l_2|\hat{U}'|n_il_i, n_1l_1\rangle + \left(\sum_{\substack{n_4>F\\ n_5=n_1}} - \sum_{\substack{n_5>F\\ n_6=n_1}}\right) \frac{\langle n_3l_3, n_6l_6|\hat{\Gamma}|n_il_i, n_5l_5\rangle\langle n_5l_5, n_2l_2|\hat{U}|n_6l_6, n_1l_1\rangle}{\omega-(E_{n_6}-E_{n_5})+i\delta(1-2n_{n_6})}. \quad (4)$$

Here the matrix element $\langle\hat{U}'\rangle$ has two different hole states in contrast to $\langle U\rangle$. The effective interaction $\langle\Gamma\rangle$ from (4) is sought in perturbation theory of the first order with respect to the intershell interaction $\langle\hat{U}'\rangle$. Equation (4) is shown graphically in Fig. 2.

A formula analogous to (3) can be written for the cross section $\sigma^{(\nabla)}$ whose dipole matrix elements are evaluated using the momentum operator $\hat{\nabla}$[6]. It is well known that for exact wave functions, just as in the RPAE approximation (taking into account all the hole states)[3] the cross sections $\sigma^{(r)}$ and $\sigma^{(\nabla)}$ must coincide. Therefore in order to check and control the numerical accuracy we have calculated the cross section both with the operator $\hat{r}$ and with the operator $\hat{\nabla}$.

3. CHOICE OF SINGLE-PARTICLE WAVE FUNCTIONS

In determining the matrix elements appearing in equations (2)–(4) we utilize the Hartree-Fock wave functions $|nl\rangle$ of an electron with quantum numbers n, l, m, s:

$$|nl\rangle \equiv \varphi_{nlm_s} = r^{-1}P_{nl}(r)\,Y_{lm}(\theta, \varphi)\chi_s. \quad (5)$$

The wave functions for the ground state of the atom are in one-configuration Hartree-Fock approximation. The complete wave function of the final state of the atom is described by a linear combinatinn of Slater determinants corresponding to definite values of total orbital angular momentum L and spin S. The single-particle wave functions of excited states in the field of the singly ionized ion are obtained from the equation

$$\left(-\frac{\nabla^2}{2}-\frac{Z}{r}+\sum_{\substack{j\leqslant F\\ j\neq i}}\int\frac{\varphi_j^*(\mathbf{r}')\varphi_j(\mathbf{r}')\,d\mathbf{r}'}{|\mathbf{r}-\mathbf{r}'|}\right)\varphi_n(\mathbf{r}) - \sum_{\substack{j\leqslant F\\ j\neq i}}\delta_{s_js_n}\int\frac{\varphi_j^*(\mathbf{r}')\varphi_n(\mathbf{r}')\,d\mathbf{r}'}{|\mathbf{r}-\mathbf{r}'|}\varphi_j(\mathbf{r}) = E_n\varphi_n(\mathbf{r}) + \sum_{j\leqslant F}\varphi_j(\mathbf{r})\langle j, i|\hat{U}|i, n\rangle, \quad (6)$$

where i is the state in which the electron existed prior to the transition to the excited level (i is the set of quantum numbers n, l, m, s). This equation determines the wave functions which take into account that portion of the diagrams of the RPAE method which refers to processes directed "forward in time" (i.e., each subsequent interaction occurs later than the preceding one) and diagonal with respect to the hole state[3]. In order to avoid taking the same processes into account twice appropriate matrix elements were excluded in solving equations (2) and (4). The last term on the right hand side of equation (6) guarantees orthogonality of wave functions of excited states to wave functions of occupied states. The use of nonorthogonalized functions in calculations of photoabsorption is equivalent to taking into account additional diagrams going outside the framework of RPAE (Fig. 3a and b), including those which have have no physical meaning from the point of view of many-body theory (Fig. 3c). In the latter the interaction with the field U created by the hole i occurs earlier than the latter has appeared. But the specific property of the field with which the hole acts on the emerging electron is that it is created simultaneously with the ejection of the electron, i.e., it is switched on suddenly at the instant when the quantum "gives birth" both to the electron and the hole.

As concrete calculations have shown, orthogonalization of wave functions leads to changes in dipole matrix elements which attain values of 10–30%, and this is significant in the set of phenomena under investigation.

4. DETAILS OF CALCULATIONS

For the calculations it is necessary to know the dipole matrix elements for the photoeffect and the matrix elements for the effective interaction between the electrons taking into account correlations within the framework of a single transition. Moreover, the amplitude contains integration over intermediate states for the carrying out of which it is necessary to know the matrix elements for the given quantum energy ω and for different energies of the emerging electron. In the

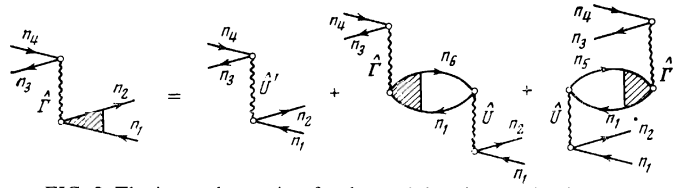

FIG. 2. The integral equation for determining the matrix element of the intershell interaction $\langle\hat{\Gamma}\rangle$ with correlations within the framework of the $n_1l_1 \to n_2l_2$ transition.

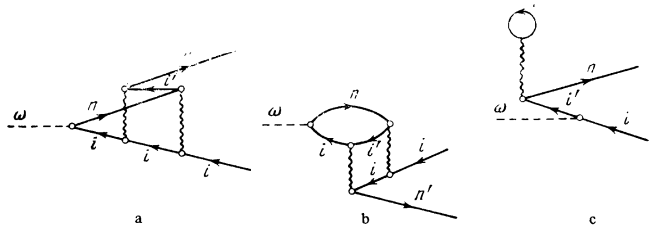

FIG. 3. Additional diagrams taken into account in calculations with a nonorthogonal wave function.

language of many-body theory this indicates evaluation of matrix elements not only on the mass surface, i.e., for $\omega = E_{n2} - E_{n1}$ (Fig. 1) but also off the surface. In solving equation (3) summation was carried out over discrete excited states and integration was carried out over the continuous spectrum. The number of discrete excitations included varied from two to five depending on the rate of falling off of oscillator strengths with increasing principal quantum number. The integral over the continuous spectrum was replaced by a sum which was cut off at a certain sufficiently high value of the energy. When a pole occurred in the integrand of equation (3) the usual formulas for numerical integration were applied to the difference not containing a pole:

$$f(x) - r/(x - x_i), \qquad (7)$$

where r is the residue of the integrand f(x) at the pole x_i.

A special set of programs has been developed in order to carry out the present calculations. In the first instance it includes programs for the calculation of wave functions of the ground state and of the excited states of the discrete and the continuous spectra in the Hartree-Fock approximation. Then the wave functions thus obtained are utilized for the calculation of the required matrix elements appearing in (3). There is available a program for the calculation of dipole matrix elements and the photoabsorption cross section both in the single-particle approximation and also in RPAE. For the determination of the latter Coulomb matrix elements are found which are diagonal with respect to the hole state, and then equation (2) is solved which then determines the matrix elements of the photoeffect including the correlations which appear in (3). The matrix elements of the effective intershell interaction with correlations within the framework of a single transition are evaluated with the aid of equation (4). In view of integration over the virtual excited states the dipole matrix elements of the intershell interaction with correlations are calculated off the mass surface. Moreover, a number of auxiliary programs was produced which enabled us to automate the different calculations up to carrying out one-dimensional integrals. This set of programs can be utilized in different combinations, and this enables us also to study many processes in atoms which are not considered in the present paper. The calculations were carried out on BÉSM-4 and BÉSM-6 machines.

5. THE PHOTOIONIZATION CROSS SECTION OF OUTER ns^2-SUBSHELLS OF NOBLE GAS ATOMS

We have carried out calculations of the photoionization cross section for the ns^2 subshells of Ne, Ar, Kr and Xe, where n is the principal quantum number of the outer shell, both in the Hartree-Fock[1)] approximation and in RPAE.

The effect of the np^6 subshell was taken into account by means of formula (3) in which virtual excitations of the form $np^5\epsilon' d$[4] were taken into account, where ϵ' is the electron energy. The effect of correlations inside the s^2 subshells does not exceed 1%. Therefore the first term in (3) was taken in the Hartree-Fock approximation, while the matrix element of the intershell interaction was taken in the form $\langle \hat{U}' \rangle$ from (4). The second term in the amplitude (the correlation amplitude) appearing in (3) has a real and an imaginary part. As a result of calculations it turns out that the real part of the correlation amplitude for Ar, Kr, and Xe atoms near the ionization thresholds of the ns^2 subshells exceeds by severalfold in absolute value the amplitude for direct ejection of s electrons (the first term of (3)) and has the opposite sign. With increasing energy ω of the γ quantum both the real and imaginary parts of the correlation amplitude fall off rapidly. At an energy at which the zero order amplitude and the real part of the correlation amplitude become comparable in absolute value the real part of the total amplitude vanishes. At the same energy the imaginary part of the amplitude is also close to zero[2)].

In Figs. 4, 5, and 6a results are given of calculations respectively for Kr, Xe and Ar where σ_r^0 and σ_∇^0 are single-particle cross sections calculated using the operators $\hat{r}$ and $\hat{\nabla}$, while σ is the cross section obtained taking into account the effect of the np^6 subshell. The effect of two simultaneous transitions on the photoionization cross section for ns^2: $np \to \epsilon' d$ and $np \to \epsilon' s$ was taken into account. The correlation amplitude in (3) in this case in turn consisted of two terms each of which described the effect of one transition on the observed one $ns \to \epsilon p$. We note that the principal contribution to the correlation amplitude is given by the term which takes into account the $np \to \epsilon' d$ transition, and it is the one determining the behavior of the cross section near the threshold[4]. The effect of the $np \to \epsilon' s$ transition acts in the same direction, as the effect of the $np \to \epsilon' d$ transition, but its contribution to the correlation amplitude is small and in the near-threshold region

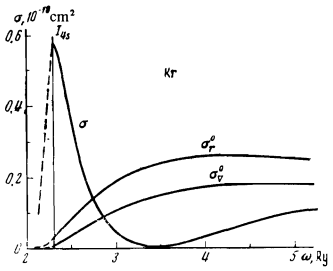

FIG. 4

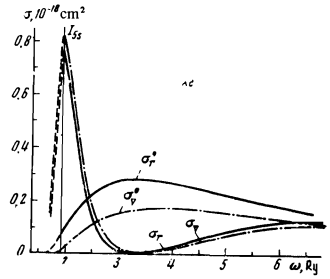

FIG. 5

FIG. 4. The photoionization cross section for the $4s^2$ subshell of Kr, σ_r^0 and σ_∇^0 are the cross sections in the Hartree-Fock approximation, σ is the cross section taking into account the effect of the $4p^6$ subshell.

FIG. 5. The photoionization cross section for the $5s^2$ subshell in Xe. σ_r and σ_∇ are the cross sections taking into account the effect of the $5p^6$ subshell obtained using the operators $\hat{r}$ and $\hat{\nabla}$.

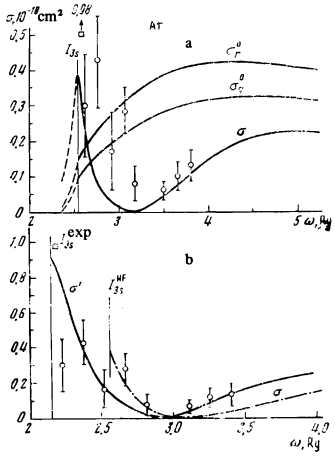

FIG. 6. The photoionization cross section for the $3s^2$ subshell in Ar, where σ is the cross section taking into account the effect of the $3p^6$ subshell; a) experimental points have been adjusted to the calculated threshold; b) comparison of the results of calculations of the cross sections σ' using the experimental threshold and σ using the calculated threshold. The experimental data are taken from [1,8].

amounts to $\lesssim 10\%$. The results of calculations with the operators $\hat{r}$ and $\hat{\nabla}$ practically coincide over the whole energy region. In order to obtain an idea of the scale of the difference between the cross sections σ_r and σ_∇ both curves are given in Fig. 5 for the Xe atom where the difference is the greatest.

As can be seen from Figs. 4, 5, and 6a the effect of the np^6 subshell has radically altered the behavior of the photoionization cross section for the ns^2 subshells. The role played by the correlations is particularly great in the energy region close to the ionization threshold, i.e., in the region where the interaction between the subshells is the greatest. It is natural to expect that the oscillator strengths of excited discrete states $ns^1np^6n'p$ will also significantly change under the influence of the np^6 subshell. In Table I calculations are presented of the oscillator strengths of certain excited levels in Ar and Kr in the Hartree-Fock approximation with the intershell interaction also taken into account. As can be seen, in certain cases the difference between the results of the two calculations reaches an order of magnitude.

The physical explanation of such behavior of the photoabsorption cross section consists of the fact that the many-electron outer shell effectively screens the more deeply lying ns^2 from the external electromagnetic field, with the amount of screening being dependent on the frequency of the incident quantum. At low energies (close to the threshold of the ns^2 subshell) the incident electromagnetic field "sets into oscillation" the outer electron subshell which as a result of its strong coupling to the inner ns^2 subshell ejects its electrons into the continuous spectrum. Near the ionization threshold the whole process is determined by the effect of the np^6 subshell. With increasing frequency of the quantum the interaction between the subshells diminishes, the "in-phaseness" of the oscillations of the electrons of the p and s subshells is destroyed and at a certain characteristic frequency when the oscillations are out of phase the ionization cross section has a minimum value. As the energy increases further the outer shell becomes more and more "transparent" for the incident radiation and the photoabsorption cross section approaches the value determined by the direct interaction of the radiation with the s electrons.

In the case of the Ar atom there exist experimental data regarding the partial contribution of the $3s^2$ subshell shell to the photoionization cross section. There is available one point at the very threshold[8] and a number of points given in reference[1] which had as its aim the detection of the minimum in the ionization cross section for the $3s^2$ subshell predicted in[4]. As can be seen from Fig. 6a experiment qualitatively confirms this supposition. However, in making comparison with experiment the calculated Hartree-Fock value of the ionization threshold $I_{3s}^{HF} = 2.555$ Ry was artificially made to coincide with the experimental value $I_{3s}^{exp} = 2.15$[9].

Taking this difference into account can significantly alter the value of the cross section near the ionization threshold as a result of the rapid variation of the total amplitude as a function of the energy ω. In order to determine the effect of the magnitude of the ionization potential on the curve for the photoabsorption cross section a calculation was also carried out using the experimental value $I_{3s}^{exp} = 2.15$ Ry. In Fig. 6b, a comparison is made of the results of the calculations using the experimental and the Hartree-Fock values for the ionization potential. We note that the greatest changes took place in the near-threshold region. If one makes comparisons in the energy scale of the ejected electron, then the calculation using the experimental value I_{3s}^{exp} shifts the whole cross section curve in the direction of higher energies. Agreement with experimental data is improved.

In contrast to the Ar, Kr, and Xe atoms in the case of Ne the correlation amplitude exerts less influence on the photoabsorption cross section for the $2s^2$ subshell. As can be seen from Fig. 7 taking the intershell interaction into account led to the result that the photoabsorption cross section was diminished by 20–30% compared to the single-particle value. The difference between Ne and the other noble gas atoms consists of the fact that correlations within the framework of the $2p^6$ subshell are comparatively weak[3]. In accordance with this the effect of $2p^6$ on the photoionization of $2s^2$ is also small compared to the effect of the p^6 subshells in other atoms. In Fig. 7 results are also shown of an experiment recently carried out[10] which completely agree with our calculations.

6. THE PHOTOIONIZATION CROSS SECTION FOR THE $4s^2$ SUBSHELLS IN Ca AND Zn

We consider the photoionization of the outer $4s^2$ subshell in Ca and Zn and the effect on its cross section exerted by the more deeply lying $3p^6$ and $3d^{10}$ subshells in Ca and Zn respectively. The specific features in this case consist of the fact that quantum energies are considered up to the ionization threshold of the inner shells. Thus, when integrations over virtual excitations are carried out in expression (3) in the correlation amplitude the denominator nowhere vanishes.

The results of calculations of the photoionization cross section for the $4s^2$ subshells in Ca and Zn in the Hartree-Fock approximation bring out a considerable difference compared to the behavior of the cross sections for the s subshells of noble gas atoms obtained in the same approximation. In Figs. 8a and 9a are shown the available experimental data[11,12] on photo-

TABLE I. Oscillator strengths for the discrete excitations of outer s^2-subshells in Ar and Kr.

		f^{HF}		f	
		$\hat{r}$	$\hat{\nabla}$	$\hat{r}$	$\hat{\nabla}$
Ar	$3s^13p^64p$	0.0017	$9.1\cdot10^{-4}$	0.011	0.012
	$3s^13p^65p$	$8.1\cdot10^{-4}$	$4.6\cdot10^{-4}$	0.003	0.003
	$3s^13p^66p$	$4.1\cdot10^{-4}$	$2.3\cdot10^{-4}$	0.0013	0.0013
Kr	$4s^14p^65p$	$8.6\cdot10^{-5}$	$6.0\cdot10^{-6}$	0.012	0.014
	$4s^14p^66p$	$1.1\cdot10^{-4}$	$9.7\cdot10^{-6}$	0.0038	0.0042
	$4s^14p^67p$	$7.0\cdot10^{-5}$	$1.0\cdot10^{-5}$	0.0017	0.0019

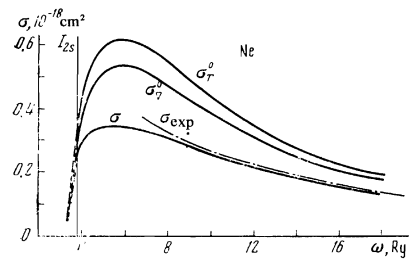

FIG. 7. The photoionization cross section for the $2s^2$ subshell in Ne. σ is the cross section taking the $2p^6$ subshell into account. The experimental data have been taken from [10].

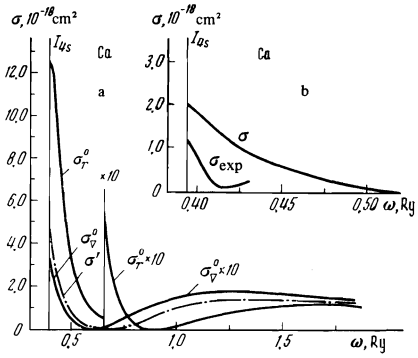

FIG. 8. The ionization cross section for the $4s^2$ subshell in Ca: a) σ' is the cross section taking into account the correlations within the framework of the $4s^2$ subshell; b) σ is the cross section taking into account the effect of the $3p^6$ subshell. Experimental data have been taken from [11].

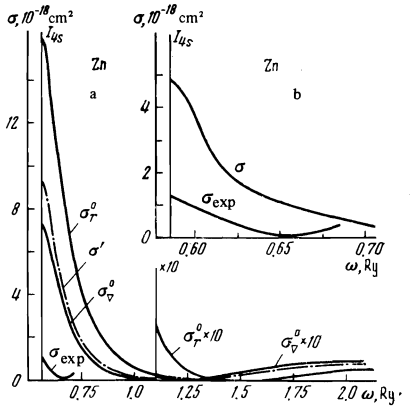

FIG. 9. The photoionization cross section for the $4s^2$ subshell in Zn: a) σ' is the cross section taking into account correlations within the framework of the $4s^2$ subshell; b) σ is the cross section taking into account the effect of the $3d^{10}$ subshell. Experimental data have been taken from [12].

absorption in Ca and Zn together with the calculated cross sections, both the single-particle ones, and those obtained in the RPAE approximation within the framework of the $4s^2$ subshell. The single-particle cross sections $\sigma^0_{\hat{r}}$ and $\sigma^0_{\hat{\nabla}}$ calculated using the operators $\hat{r}$ and $\hat{\nabla}$ differ significantly both from each other and also (and even to a greater extent) from experiment. The correlations within this subshell manifest themselves significantly more strongly than in the case of the s^2 subshells in noble gas atoms where they practically do not alter the results of the single-particle calculation. But in the case of Ca and Zn the difference between the cross sections $\sigma'_{\hat{r}}$ and $\sigma'_{\hat{\nabla}}$ calculated in the RPAE with the operators $\hat{r}$ and $\hat{\nabla}$ becomes small, however, the deviation from experiment at the threshold remains considerable (approximately by a factor of 4). A calculation for Ca using the coordinate operator taking into account the RPAE correlations within the framework of the $4s^2$ shell has been carried out earlier by Altick and Glassgold[13]. Our result has turned out to be close to that given in[13] even though Altick and Glassgold carried out their calculations not in a self-consistent manner.

The effect of the $3p^6$ and $3d^{10}$ subshells in Ca and Zn respectively on the photoionization of the $4s^2$ subshell was investigated. Since the correlations are large both for the electrons, and also for the electrons of the inner shells, the calculation was carried out in accordance with formula (3) without additional approximations. It turned out that taking into account the effect of the inner shells leads to a significant decrease in the cross section at the threshold and improves agreement with experiment (Figs. 8b and 9b). In this case one can not limit oneself to taking into account the effect of only one transition in the inner shell. The contributions of both transitions $3d \to \epsilon'f$ and $3d \to \epsilon'p$ for Zn are of the same order of magnitude in contrast to the case with the transitions $np \to \epsilon'd$ and $np \to \epsilon's$ in np^6 subshells in noble gas atoms. The correlation amplitude appearing in (3) consisted of two terms describing in the first order of perturbation theory in terms of the intershell interaction the effect of both transitions on photoionization of $4s^2$.

As can be seen from Figs. 8b and 9b there still remains the difference of the calculated cross section σ from the experimental one. This difference is possibly associated with the fact that the theoretical Hartree-Fock values of the ionization thresholds differ from the experimental ones. For the outer $4s^2$ subshell this difference amounts to[9] 0.06 Ry in Ca and 0.11 Ry in Zn, while for the inner $3p^6$ in Ca it amounts to 0.62 Ry and for the $3d^{10}$ in Zn it amounts to 0.73 Ry.

In Table II are given oscillator strengths for several excited states of the form $4s^1np$ in Ca and Zn f^{HF} calculated in the Hartree-Fock approximation and f taking correlations into account both within the shell, and under the influence of the inner shell. Inclusion of the intershell interaction leads to good agreement with experiment[14-16].

7. CROSS SECTION FOR THE SINGLE IONIZATION OF Kr AND Xe ATOMS NEAR THE THRESHOLDS OF THE d^{10}-SUBSHELLS

We consider the effect of a many-electron deep shell near its ionization threshold on the photoabsorption in outer shells.

In experiments on photoionization[17,18] a significant increase was observed in the number of singly charged ions near the threshold of the $4d^{10}$ shell in Xe and to a lesser degree near the threshold of the $3d^{10}$ shell in Kr. The direct photoionization of the d^{10} subshells practically gives no yield of singly charged ions due to the dominant contribution of the Auger-process which leads to the state of the doubly charged ion. On the other hand the cross section for photoionization with the simultaneous excitation of the atom to a discrete level, as is shown by estimates, and the cross section for the direct photoionization of the outer shell ns^2np^6 are too small in magnitude. Thus, for Xe the latter is by an order of magnitude smaller than the experimental cross section for single photoionization σ^+ and does not have a maximum in this region.

It has turned out that the mechanism responsible for the increase in σ^+ is associated with the intershell interaction, and, in particular, with the effect of the $(n-1)d^{10}$ subshell on the photoionization of the outer ns^2np^6. The calculation was also carried out with the aid of formula (3). The effect was taken into account of only one $(n-1)d \to \epsilon'f$ transition (within which correlations were taken into account within the framework of the RPAE). The total cross section was made up of three partial

TABLE II. Oscillator strengths for the discrete excitations of the $4s^2$ shells in Ca and Zn.

		f^{HF}		f	Experiment Ca[14,15] Zn[16]
		$\hat{r}$	$\hat{\nabla}$		
Ca	$4s^14p$	2.52	1.23	1.81	1.75
	$4s^15p$	0.35	0.13	0.16	0.20
	$4s^16p$	0.095	0.031	0.035	0.043
Zn	$4s^14p$	1.94	1.16	1.50	1.46
	$4s^15p$	0.31	0.16	0.14	—
	$4s^16p$	0.096	0.047	0.028	—

cross sections calculated according to (3) and relating to transitions in the outer shell np → εd, np → ε, ns → εp. All these three transitions within the energy region under consideration make contributions to the photoionization cross section of the same order of magnitude. In Fig. 10 calculated cross sections are shown for the photoionization of outer shells of Xe and Kr in the neighborhood of the thresholds of the d^{10} subshells: σ^0 obtained in the single-particle approximation and σ taking into account the effect of the (n − 1)d → ε'f transition, and also experimental data[17,18] are shown. In view of the small deviation of σ_r from σ_∇ average curves are given in Fig. 10. Taking into account the effect of many-electron d^{10} subshells leads to an essential change in the result of the single-particle calculation. For the Kr atom this effect turned out to be the smaller one (Fig. 10b). Thus, on comparing Fis. 10a and 10b one can note that $4d^{10}$ exerts an incomparably greater effect on the photoionization of the outer shell than does $3d^{10}$. We note that the correlation within the $4d^{10}$ subshell in Xe is stronger than in the $3d^{10}$ subshell in Kr[3]. On the other hand the smaller value of the dipole matrix element for $3d^{10}$ and the greater energy gap (compared to Xe) separating $3d^{10}$ from the outer shell, —all this also leads to a decrease of the correlation effect of $3d^{10}$ in Kr.

The results of such calculations exhibit qualitative agreement with the available experimental data (Fig. 10). However, the error in the experimental data, and likewise differences between them[17,18] are great.

The effect of the inner $2p^6$ subshell in Ar on the yield of singly charged ions turns out not to be significant. This is associated with the large value of the energy gap separating it from the outer shell, and also with the weakness of its correlations within the $2p^6$ subshell.

As an example results are given in Fig. 11 of calculations of cross sections of partial transitions 5p → εd and 5s → εp in Xe both in the single-particle approximation, and taking the 4d → ε'f transition into account. The greatest effect of the correlation amplitude is manifested in the case of the 5p → εd transition which has a Cooper minimum near the ionization threshold for the $4d^{10}$ subshell. Figure 11 shows σ_r and σ_∇ in order to illustrate the difference between them. The smallest effect of the correlation term in (3) was exhibited in the case of the 5p → εs transition, but even in that case the difference at the maximum between σ^0 and σ amounts to a factor of 2—2.5. In the case of the Kr atom the effect of the $3d^{10}$ subshell is most strongly pronounced for the 4p → εd transition.

It is essential to note that the photoionization cross sections for the $4s^2$ subshell in Kr and the $5s^2$ subshell in Xe have a characteristic shape. Near the ionization threshold their behavior is determined by the effect of the outer p^6 subshell, and this is reflected in the appearance of a deep minimum immediately beyond the threshold. At high energies this influence is at first compensated by the effect of the inner d electrons and is then completely determined by it, leading to a maximum near the threshold of the d^{10} subshell.

8. CONCLUSION

In the present paper we have studied the effect of strong transitions on weak ones. In order to elucidate the question concerning the interaction of two strong

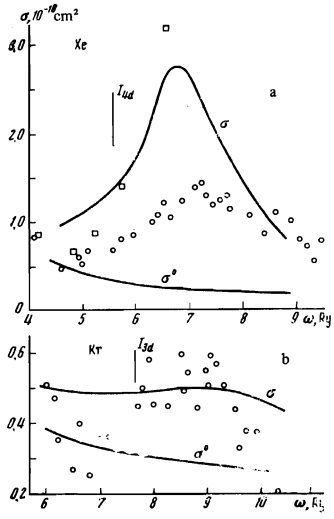

FIG. 10.

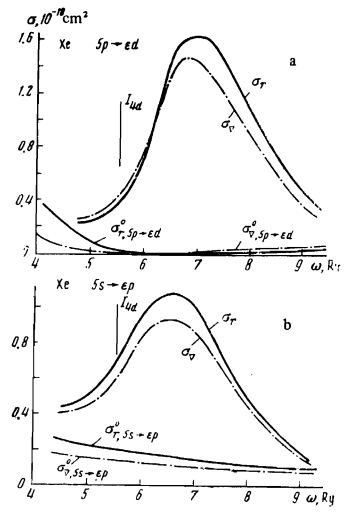

FIG. 11

FIG. 10. The cross section for the yield of singly charged ions in Xe and Kr: a) Xe, σ is the cross section taking into account the effect of the $4d^{10}$ subshell; b) Kr, σ is the cross section taking into account the $3d^{10}$ subshell. Experimental data: □ from [17], ○ from [18].

FIG. 11. Contribution of the partial transitions to the cross section for single ionization of Xe: a) σ_r and σ_∇ are the cross sections for the 5p → εd transition taking into account the effect of 4d → ε'f obtained with the operators $\hat{r}$ and $\hat{\nabla}$; b) σ_r and σ_∇ are the cross sections for the 5s → εp transition taking into account the effect of the 4d → ε'f transition.

transitions we have considered the effect of the $4d^{10}$ subshell on the $4p^6$ subshell in Pd and Xe. Taking it into account leads to an increase in the photoionization cross section for the $4p^6$ subshell in Pd near the threshold while in Xe it leads to the appearance of a minimum similar to the minimum for the ns^2 subshells of Ar, Kr and Xe atoms. Within the framework of the $4d^{10}$ subshell itself in Pd the correlations are just as great, while the interaction of the transitions 4d → εf and 4d → εp decreases the probability of the latter by a factor of two.

On the basis of the examples given above one can conclude that the effect of the intershell interaction must be taken into account in all cases when a many-electron shell, having a strong (main) transition with strong correlations within it, is situated in the immediate neighborhood of the shell under consideration.

[1)] A calculation in a somewhat inconsistent Hartree-Fock approximation has been carried out in [7]. The results of their and our single-particle calculations turned out to be close to each other.

[2)] It is quite possible that when the real part of the total amplitude vanishes the imaginary part must also vanish at the same energy.

[1] M. J. Lynch, A. B. Gardner, K. Codling and G. V. Marr, Phys. Lett. 43A, 237 (1973).

[2] U. Fano and J. W. Cooper, Rev. Mod. Phys. 40, 441 (1968).

[3] M. Ya. Amus'ya, N. A. Cherepkov and L. V. Chernysheva, Zh. Eksp. Teor. Fiz. 60, 160 (1971) [Sov. Phys.-JETP 33, 90 (1971)].

[4] M. Ya. Amusia, V. K. Ivanov, N. A. Cherepkov and L. V. Chernysheva, Phys. Lett. 40A, 361 (1972).

[5] M. Ya. Amusia, L. V. Chernysheva and V. K. Ivanov, Phys. Lett. 43A, 243 (1973).

[6]I. I. Sobel'man, Vvedenie v teoriyu atomnykh spektrov (Introduction to the Theory of Atomic Spectra), Fizmatgiz, 1963.
[7]D. J. Kennedy and S. T. Manson, Phys. Rev. **A5**, 227 (1972).
[8]J. A. R. Samson and R. B. Cairns, Phys. Rev. **173**, 80 (1968).
[9]W. Lotz, J. Opt. Soc. Am. **60**, 206 (1970).
[10]F. Wuilleumier and M. O. Krause, Electronic and Atomic Collisions (VIII ICPEAC) Abstract of Papers, Beogard, 1973, p. 569.
[11]V. L. Carter, R. D. Hudson and B. L. Breig, Phys. Rev. **A4**, 821 (1971).
[12]G. V. Marr and J. M. Austin, J. Phys. **B2**, 107 (1969).
[13]P. L. Altick and A. E. Glassgold, Phys. Rev. **133**, A632 (1964).
[14]W. H. Smith and M. S. Liszt, J. Opt. Soc. Am. **61**, 938 (1971).
[15]W. L. Wiese, M. W. Smith and B. M. Miles, Atomic Transition Probabilities, **2**, Sodium through calcium, NSRDS-NBS 22, Oct. 1969.
[16]A. Lurio, R. L. DeZafra and R. J. Goshen, Phys. Rev. **134**, A1189 (1964).
[17]R. B. Cairns, H. Harrison and R. I. Schoen, Phys. Rev. **183**, 52 (1969).
[18]T. M. El-Sherbini and M. J. Van der Wiel, Physica **62**, 119 (1972).

Translated by G. Volkoff
158